Lecture Notes in Electrical Engineering 399

Canjun Yang
G.S. Virk
Huayong Yang
Editors

Wearable Sensors and Robots

Proceedings of International Conference on Wearable Sensors and Robots 2015

ZHEJIANG UNIVERSITY PRESS
浙江大学出版社

Springer

Lecture Notes in Electrical Engineering

Volume 399

Board of Series editors

Leopoldo Angrisani, Napoli, Italy
Marco Arteaga, Coyoacán, México
Samarjit Chakraborty, München, Germany
Jiming Chen, Hangzhou, P.R. China
Tan Kay Chen, Singapore, Singapore
Rüdiger Dillmann, Karlsruhe, Germany
Haibin Duan, Beijing, China
Gianluigi Ferrari, Parma, Italy
Manuel Ferre, Madrid, Spain
Sandra Hirche, München, Germany
Faryar Jabbari, Irvine, USA
Janusz Kacprzyk, Warsaw, Poland
Alaa Khamis, New Cairo City, Egypt
Torsten Kroeger, Stanford, USA
Tan Cher Ming, Singapore, Singapore
Wolfgang Minker, Ulm, Germany
Pradeep Misra, Dayton, USA
Sebastian Möller, Berlin, Germany
Subhas Mukhopadyay, Palmerston, New Zealand
Cun-Zheng Ning, Tempe, USA
Toyoaki Nishida, Sakyo-ku, Japan
Bijaya Ketan Panigrahi, New Delhi, India
Federica Pascucci, Roma, Italy
Tariq Samad, Minneapolis, USA
Gan Woon Seng, Nanyang Avenue, Singapore
Germano Veiga, Porto, Portugal
Haitao Wu, Beijing, China
Junjie James Zhang, Charlotte, USA

About this Series

"Lecture Notes in Electrical Engineering (LNEE)" is a book series which reports the latest research and developments in Electrical Engineering, namely:

- Communication, Networks, and Information Theory
- Computer Engineering
- Signal, Image, Speech and Information Processing
- Circuits and Systems
- Bioengineering

LNEE publishes authored monographs and contributed volumes which present cutting edge research information as well as new perspectives on classical fields, while maintaining Springer's high standards of academic excellence. Also considered for publication are lecture materials, proceedings, and other related materials of exceptionally high quality and interest. The subject matter should be original and timely, reporting the latest research and developments in all areas of electrical engineering.

The audience for the books in LNEE consists of advanced level students, researchers, and industry professionals working at the forefront of their fields. Much like Springer's other Lecture Notes series, LNEE will be distributed through Springer's print and electronic publishing channels.

More information about this series at http://www.springer.com/series/7818

Canjun Yang · G.S. Virk · Huayong Yang
Editors

Wearable Sensors and Robots

Proceedings of International Conference on Wearable Sensors and Robots 2015

ZHEJIANG UNIVERSITY PRESS
浙江大学出版社

Springer

Editors
Canjun Yang
Department of Mechanical Engineering
Zhejiang University
Hangzhou, Zhejiang
China

Huayong Yang
Department of Mechanical Engineering
Zhejiang University
Hangzhou, Zhejiang
China

G.S. Virk
University of Gävle
Gävle
Sweden

ISSN 1876-1100 ISSN 1876-1119 (electronic)
Lecture Notes in Electrical Engineering
ISBN 978-981-10-2403-0 ISBN 978-981-10-2404-7 (eBook)
DOI 10.1007/978-981-10-2404-7

Jointly published with Zhejiang University Press, Hangzhou, China

Library of Congress Control Number: 2016947751

© Zhejiang University Press and Springer Science+Business Media Singapore 2017
This work is subject to copyright. All rights are reserved by the Publishers, whether the whole or part of the material is concerned, specifically the rights of translation, reprinting, reuse of illustrations, recitation, broadcasting, reproduction on microfilms or in any other physical way, and transmission or information storage and retrieval, electronic adaptation, computer software, or by similar or dissimilar methodology now known or hereafter developed.
The use of general descriptive names, registered names, trademarks, service marks, etc. in this publication does not imply, even in the absence of a specific statement, that such names are exempt from the relevant protective laws and regulations and therefore free for general use.
The publishers, the authors and the editors are safe to assume that the advice and information in this book are believed to be true and accurate at the date of publication. Neither the publishers nor the authors or the editors give a warranty, express or implied, with respect to the material contained herein or for any errors or omissions that may have been made.

Printed on acid-free paper

This Springer imprint is published by Springer Nature
The registered company is Springer Science+Business Media Singapore Pte Ltd.

Preface

The International Conference on Wearable Sensors and Robots (ICWSR 2015) held during October 16–18, 2015 in Hangzhou, China. ICWSR 2015 was sponsored by Zhejiang University, and co-sponsored by the National Natural Science Fund of China (NSFC), and International Organisation for Standardisation's working group on personal care robot safety (ISO/TC184/SC2/WG7).

With rapid progress in mechatronics and robotics, wearable sensing and robotic technologies have been widely studied for various applications including exoskeleton robots for rehabilitation, exoskeleton robots for supporting the daily lives of elderly people, wearable medical devices for monitoring vital signs, etc. However, some key technology challenges need to be addressed for achieving better research results, more effective application demonstrators and realistic commercialization. The conference brought together academics, researchers, engineers, and students worldwide to focus on and discuss the state of the art of the technology and to present the latest results on the various aspects of wearable sensors and robots.

The conference received 61 papers from experts and researchers in China and all over the world. 46 papers were reviewed and accepted, including 20 invited papers and 26 general papers. Meanwhile, the conference received 11 keynote speech abstracts from international professors and researchers. The proceedings consist of detailed papers on wearable sensors, design of sensors and actuators, advanced control systems, wearable robots, visual recognition applications, clinical applications, rehabilitation robotics, biological signal based robotics, intelligent manufacturing and industry robots, and research progress from keynote speakers. In addition, readers will obtain the latest information on medical device regulation and international standardization, wearable robots for training and support of human gait, design of exoskeleton for elderly persons, ergonomics design considerations driving innovation in assistive robotics, and analysis of human–machine interaction.

It is our desire that the proceedings of the International Conference on Wearable Sensors and Robots (ICWSR 2015) will provide an opportunity to share the perspectives of academic researchers and practical engineers on wearable sensors and robot research and development.

Hangzhou, China
Gävle, Sweden
October 2015

Prof. Canjun Yang
Prof. G.S. Virk
Program Chair, General Chair of ICWSR 2015

Contents

Part I
Wearable Sensors

The Design of E Glove Hand Function Evaluation Device Based on Fusion of Vision and Touch

Jing Guo, Cui-lian Zhao, Yu Li, Lin-hui Luo and Kun-feng Zhang

Abstract This paper presents an E glove hand function evaluation device based on visual and haptic fusion, and uses the Principal Component Analysis (PCA) algorithm to establish hand sensor distribution model. The PCA analysis chart shows that three sensors distributed on the thumb, forefinger, and middle finger could effectively estimate the grasp motions. Moreover, threshold values for all category models can be selected by the way of adaptive pressure threshold integrating visual aid. At last, five subjects dressed E glove judging the grasp motions under different combinations of sensors. The results show that: the classification accuracy rate depended on the pressure and visual sensor fusion method reached 94 %; the identification rate of the adaptive pressure threshold method to judge the grasp motions can be increased 1.6–1.7 times than only using single camera vision sensor or pressure sensor. Next step, the E glove hand function evaluation device will be further improved such as function of active control to the collected data will be added.

Keywords E glove · PCA · Pressure sensing · Visual and touch fusion

1 Introduction

Hands are primarily responsible for the sophisticated activities and work in motor function, its degree of flexibility and movement accuracy are closely related to human activities of daily living, quality of life, and social activities. In medical rehabilitation, stroke patient hand is with motor dysfunction, and Parkinson's disease patients with hand tremors and slow movement will lead to the hand motor

J. Guo (✉) · C. Zhao · Y. Li · L. Luo · K. Zhang
Shanghai Key Laboratory of Intelligent Manufacturing and Robotics,
School of Mechatronic Engineering and Automation, Shanghai University,
Shanghai 200072, China
e-mail: andy_guojing421@163.com

© Zhejiang University Press and Springer Science+Business Media Singapore 2017

C. Yang et al. (eds.), *Wearable Sensors and Robots*, Lecture Notes in Electrical Engineering 399, DOI 10.1007/978-981-10-2404-7_1

dysfunction. i; Hand dysfunction becomes a difficult problem in rehabilitation training and medical evaluation at present (Gabriele et al. 2009).

So far, there is no unified standard for motor dysfunction in international evaluation; each method owns its emphasis, and there have not yet been a more perfect and accurate evaluation method (Meng et al. 2013; Zampieri et al. 2011). Action Research Arm Test (ARAT) is one of the commonly used test evaluation methods of hand movement function (Lyle et al. 1981). Compared with other commonly used evaluation methods, ARAT pays more attention to comprehensive hand function in daily life, and classify and quantify the type and size of grasping object. In recent years, domestic and foreign scholars have verified the reliability and validity of ARAT by using clinical case (Weng et al. 2007; Yozbatiran et al. 2008). In view of the complex hand diverse sports demand, a lot of researches have been committed to design better wearable devices and data processing methods at home and abroad. Nathan et al. (2009) designed a wearable data glove applied in auxiliary rehabilitation training in patients; angle sensors associated with the hand acquire grasp-aperture prediction model to calculate the distance between thumb and forefinger point, then the hand grasping state was defined with the distance; although the data glove device has high accuracy and stability, the data glove device must be equipped with the Activities of Daily Living Exercise Robot (ADLER) system which is huge and thus with great limitations. Jakel et al. (2010a, b, 2012) and Palm et al. (2010, 2014) and Skoglund et al. (2010) designed a wearable data glove applied in controlling mechanical arm, which utilizes pressure data of the pressure sensors, position, velocity, and acceleration data of marks on the glove to define the hand grasping state, and then control manipulator grasping; while the data glove device can reach a high level in stability and accuracy and real-time performance, 5–6 sensors and 6–8 sets of marks or even more on glove device make information processing complex and data glove with mechanical auxiliary device reduces the flexibility and practicability; besides, sole grasp pressure threshold cannot adapt to grasp kinds of project. Liang et al. (2013) and Han et al. (2012) designed an electronic nose detection device, by acquiring reasonable information through reasonably designing the number and distribution of sensors to reduce the information redundancy; but there are many sensors, and it need to reduce the number of sensors. E glove in this paper is a glove mounted with three sensors and cloth glove without mechanism. Differences from traditional data glove used to acquire sensing information, E glove can implement active control function through dealing with the data collected in the future.

Wearable data glove device applied in hand function evaluation possesses complex structure and low flexibility and practicability, aiming at motivating patients' active movement function, wearable pressure sensing data glove device based on fusion of vision data and touch data is developed in this paper. Pressure data from sensors and marks data from the glove are acquired for evaluating the hand grasping state. Combined with the actual grasp function, sensors, and marks

on this wearable pressure sensing data glove device can accomplish tracking and evaluation at the cost of lesser sensors and marks; moreover, visual feedback technology is applied to distinguish pressure threshold of various grasping models, hence it is adaptive to grasp different projects; finally, the tracking accuracy of the different sensors combination are compared.

2 Glove Pressure Sensors Distribution Design Based on Principal Component Analysis

2.1 ARAT Grasping Motion Hand Partition Experiment

The distribution of the pressure sensors is associated with the contact region between hand and object model. In this paper, grasping motion is based on the theory of ARAT. ARAT consists of four subtests: grasp, grip, pinch, and gross motor and grasping objects of ARAT all are geometric objects with standard size. Grasping motion is one of the basic movements of hand, according to different functions grasps are divided into power grasps and precision grasps (Cutkosky et al. 1989), the two parts include all dimensions of grasping objects involved in ARAT and their corresponding grasping movements in Fig. 1.

The hand area can be divided into 0–18 areas in Fig. 2.

According to grasping motion similarity, grasp motion is divided into five classifications numbered as No. 1–No. 5. Beforehand, ARAT models are painted with blue pigment and five subjects without any illness or injury are selected and familiar with the experiment process. Let each participant grasps color model as ARAT method introduced, recording contact area number of hand after each object grasped. Table 1 shows one participant's full ARAT test contact area. Count the contact frequency for each numbered 0–18 contact area, result shows in Fig. 3.

As seen in Fig. 3, the contact area corresponding to former five highest contact frequency descending order is 12, 0, 3, 6, 9.

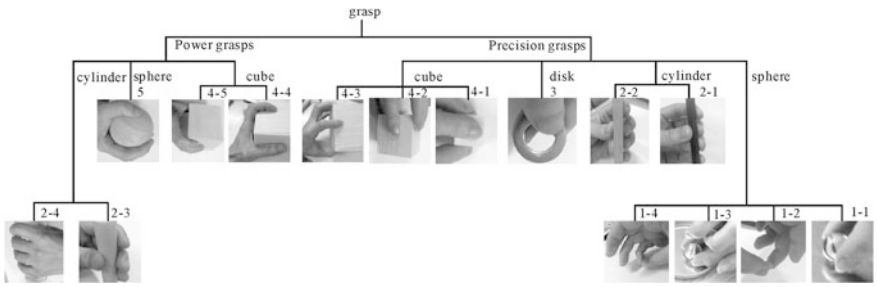

Fig. 1 Grasp classification

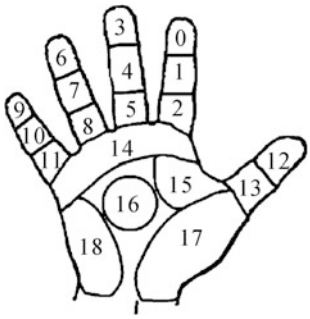

Fig. 2 Hand partition (Meng et al. 2010)

Table 1 Contact area

Grasp number	No. 1	No. 2	No. 3	No. 4	No. 5
Before grasp					
After grasp					

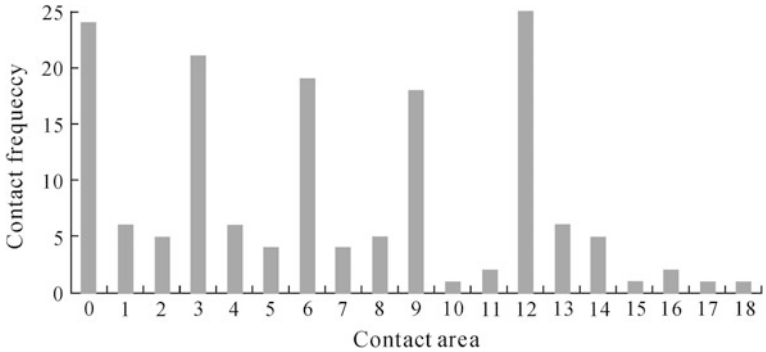

Fig. 3 Contact frequency and contact area

2.2 Sensor Layout Design Based on Principal Component Analysis

A. **Principal Component Analysis**

Principal Component Analysis (PCA) is a kind of data compression and feature information extraction technology and it converts a set of possibly correlated variables into a set of values of linearly uncorrelated variables thus reduced data

redundancy; so, the data is processed in a low-dimensional feature space and meanwhile keep most of the original data information (Li et al. 2011).

Assume a set of p data which composes a vector X: X_1, X_2,…, X_P, for each X_j (i = 1, 2,…, p) corresponding to a coefficient a variable. Reassembled a new set of unrelated number denoted as composite indicator Fm replaces original indicators. The principal component model is expression in Eq. (1)

$$\begin{cases} F_1 = a_{11}X_1 + a_{12}X_2 + \ldots + a_{1p}X_p \\ F_2 = a_{21}X_1 + a_{22}X_2 + \ldots + a_{2p}X_p \\ \quad \ldots\ldots \\ F_m = a_{m1}X_1 + a_{m2}X_2 + \ldots + a_{mp}X_p \end{cases} \tag{1}$$

(1) is denoted as $F = AX$

Where F_i is the ith principal component, i = 1, 2, ^, m; Coefficient matrix A_{ij} row vectors as unit eigenvector corresponding m eigenvalues λ_1, λ_2,..., λ_m.

B. Determine the number of sensors

It is known from experiment of Sect. 2.1 part that the contact area number with descending contact frequency is 12, 0, 3, 6, 9. Put the five-dimension pressure data in formula (1), PCA is used to reduce data dimension. Figure 4 illustrates five sensor data of grasping motion. Calculate five eigenvalues from five sensors data according to PCA algorithm model. The results are shown in Table 2.

In Table 2, principal components numbered 1–5 are the thumb, index finger, middle finger, ring finger, and little finger in turn. Table 2 demonstrates that the first three principal component's total contribution rates are 99.775 %, almost representing all the variable information. In Fig. 5, when the number of factor exceeds 3, the decrease extent of eigenvalue is very little, thus it is enough to reflect the original variable information, which implies that close last two sensors does not affect the recognition effect of grasping judgment, so the number of sensors is three, distributing in the thumb, forefinger, and middle finger fingertip position.

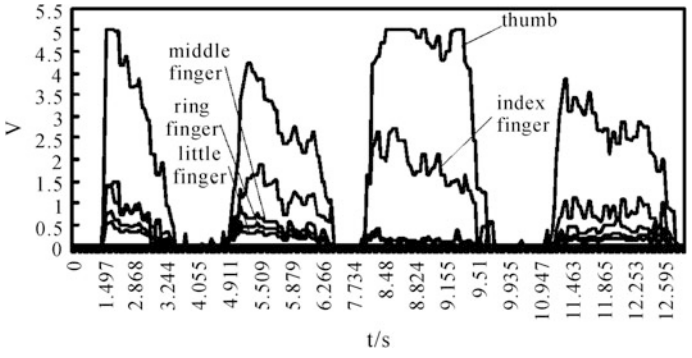

Fig. 4 Grasping action pressure distribution

Table 2 The contribution of each component of principal component analysis

Principal component number	Eigenvalue	Contribution rate (%)
1	3.9041	77.7523
2	1.0211	20.3368
3	0.0847	1.6868
4	0.0106	0.2111
5	0.0007	0.0139

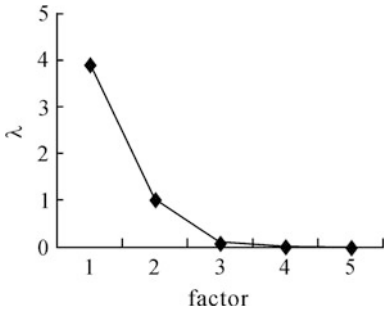

Fig. 5 Eigenvalue factor graph

3 Adaptive Pressure Threshold Acquirement Method Based on Visual Feedback

3.1 Object Detection Based on Camshift Feedback Codebook

In this paper, moving target detection algorithm-based Camshift feedback codebook model is used in visual tracking. Camshift algorithm transforms the input image into a probability distribution by target color histogram, and then calculates the moments of the target area in the transformed probability distribution. In order to achieve continuous tracking, the continuous iterative method is utilized to calculate the target rectangular window position and size, and regards the expanded rectangle window as an image processing area for the next frame. Camshift target tracking steps are as follows:

1. Initialize track objects rectangular area;
2. Extract H component images from HSV color space of each frame, and calculate the gravity position of the window;
3. Move the center of the rectangular window to the gravity position and update the rectangular window;
4. Return the rectangular window position and size of targets.

If the moving distance is greater than the convergent minimum moving distance or the number of iterations is less than the maximum number of iterations, repeat the third and fourth step until it astringes.

Camshift algorithm is mainly for tracking and recognition by identifying the color of HSV. HSV color model is a model for the user perception, focusing on color representation, including color, depth, light and shade, which can be transformed from the RGB values. In the RGB values table, the best colors can be identified are red, green, and blue. So, ARAT models are blue and marks on the wearable pressure sensor data glove are red and green. To enhance the tracking performance, marks are designed as toroidal, and red and green marks are distributed at the thumb and index fingertips.

The rectangle upper-left vertex coordinates width w_{a1} and height h_{a1} can be obtained by Camshift algorithm. The minimum of w_{a1} and h_{a1} labeled L is taken as the model of classification recognition. The computational formula is

$$L = \mathbf{min}(w_{a1}, h_{a1}) \tag{2}$$

3.2 Adaptive Pressure Threshold Acquirement

The mass of ARAT models and grasp way will affect the contact pressure threshold, so the models will be divided into three categories on the basis of model mass. Test the contact pressure threshold value for each type ARAT model. The categories are shown in Table 3 and the pressure value test is shown in Fig. 6.

The model mass has a direct relationship with the grasp pressure. The greater the mass of the model is, the larger the grasp pressure threshold. The type I grasp pressure threshold test experiments are shown in Fig. 6. A weighted fusion algorithm (Song et al. 2013) is used to normalize three fingers the pressure values. The results show that the type I contact pressure threshold is $f_1 = 0.8$. According to this algorithm, the type II contact pressure threshold is $f_2 = 0.5$, and the type III contact pressure threshold is $f_3 = 0.1$.

Table 3 ARAT object classification

TypeID	Shape	3D size (mm)
Type I	Cube	97 × 97 × 97
Type II	Cube	74 × 74 × 74
	Sphere	70 (diameter)
Type III	Cube	50 × 50 × 50
	Cube	25 × 25 × 25
	Cuboid	100 × 25 × 10
	Cylinder	200 (high) × 20 (diameter)
	Cylinder	200 (high) × 10 (diameter)
	Disk	5 (high) × 35 (diameter)
	Sphere	10 (diameter)

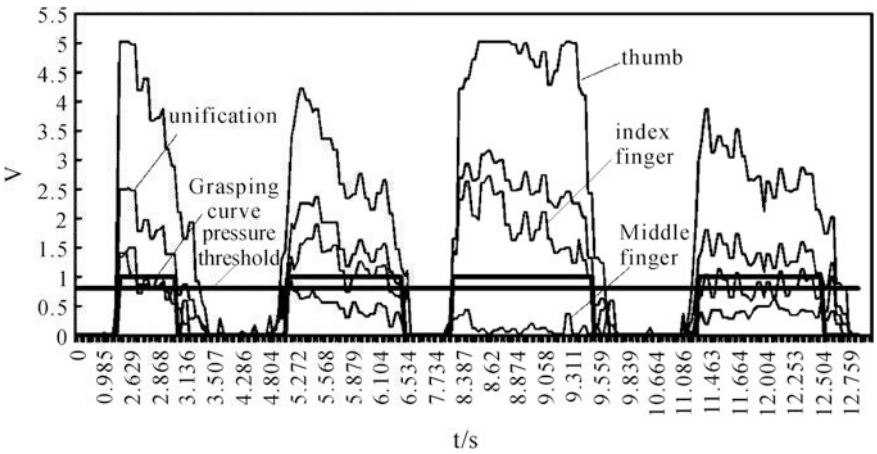

Fig. 6 Grasp pressure threshold test

The three-dimensional size of the models is directly related to the tracking rectangle. Before grasp, the model is in stationary state. According to the model rectangle achieved by target detection and the formula (2), the model belongs to which category it can be estimated. From Table 3, the rectangle threshold of the type I model is $L = 97 \pm 2$, and the type II model is $L = 70 \pm 2$. The rest of L is for the type III model. In practical application, the unit should be changed into pixel, and the value L is related to the camera installation height. Adaptive threshold for pressure calculation are as follows:

I. **Camshift**(w_{a1}, h_{a1});
CvRect(0, 0, image.cols, image.rows)
w_{a1} = image.cols
h_{a1} = image.rows
II. L = **min**(w_{a1}, h_{a1})
III. **if**($L \geq L_1$) **then** $f = f_1$

if($L \geq L_2$) **then** $f = f_2$

$f = f_3$

4 Design and Testing of Wearable Sensor Data Glove

4.1 Design of Wearable Sensor Data Glove

Wearable pressure sensor data glove is shown in Fig. 7. It includes the data acquisition part and control module encapsulated within the back side of the glove and marks encapsulated fingertip position of external part of glove and pressure

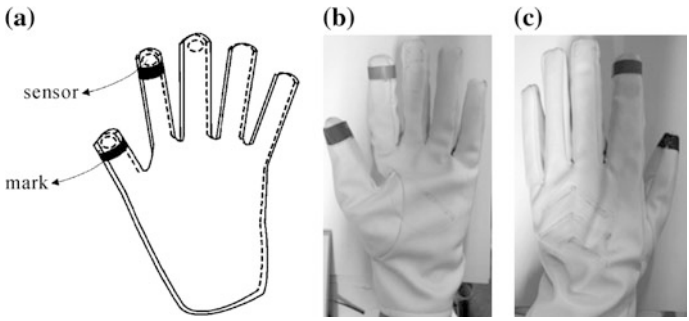

Fig. 7 Layout chart of wearable pressure sensing data glove (**a**), positive of wearable pressure sensing data glove (**b**), and back of wearable pressure sensing data glove (**c**)

sensors encapsulated in the palm side of inside the glove. Pressure sensor locates in the point where hand contacts with grasping object when hand is grasping an object.

4.2 The Analysis of the Combination of Different Sensors for Grasp Accuracy

In order to analyze the influence of the combination of different sensors for grasp accuracy, create three devices such as: single camera device, single sensors device, and combination of single camera device and single sensors device. Five subjects (No. 1–No. 5) use the above three devices to grasp the same objects. The developed software will record the visual data and the pressure data separately based on the above devices.

As shown in Fig. 8 are the grasp experiments on the condition of vision and touch fusion. Before grasp, minimum length of object rectangular is obtained through the camera, and judging object gripping pressure threshold according to rectangular threshold of object. Before the subject's hand touches object, grasp pressure is less than the grasping threshold, grasp count is 0. After grasp, hand touches object and when grasp pressure is more than the grasping threshold, at

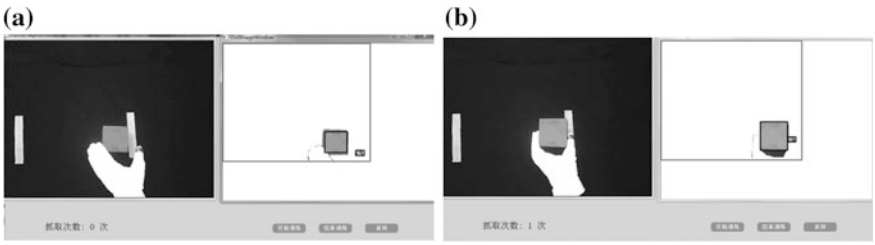

Fig. 8 Judgment number of grasp, before grasp (**a**), after grasp (**b**)

Table 4 Grasping contrast on the condition of three

	Camera	Sensor	Camera and sensor
No. 1	12	14	20
No. 2	11	10	19
No. 3	10	11	18
No. 4	13	12	18
No. 5	9	10	19
Success rate (%)	55	57	94

present grasp successful count is 1. Grasp successful counts of 5 subjects on the condition of three situations are shown in Table 4.

From the experimental result, we can know that occlusion issue is very serious on the condition of single camera device, so the success rate is lowest at 55 %; it cannot automatically adjust grasp pressure threshold without vision data when using only one grasp pressure threshold to judge all objects, so success rate is 57 %; Finally, pressure threshold cooperate with vision data to judge grasp, it can automatically adjust grasp, with a high success rate of 94 %.

5 Conclusion

An E glove hand function evaluation device based on vision and touch integration was presented in this paper, and hand sensor distribution model was established through the principal component analysis algorithm. The PCA analysis chart shows that three sensors distributed on the thumb, forefinger, and middle finger can effectively estimate the grasp motion. Moreover, it can accurately select the grasp threshold values for each category model by the adaptive pressure threshold method. Finally, five subjects dressed E glove sensors judge the grasp motion under the condition of homogeneous and heterogeneous sensors, and the highest accuracy rate of classification depended on heterogeneous sensors fusion reaches 94 %. The results show that: the identification rate of using the adaptive pressure threshold as well as vision fusion method of this simple device to judge the grasp process is better. Since the E glove hand function evaluation device is still in the laboratory stage, there are many issues worthy of further study.

Acknowledgments The authors wish to thank Dr. Zhi-jian Fan for providing guide.

References

Cutkosky MR et al (1989) On grasp choice, grasp models, and the design of hands for manufacturing tasks. IEEE Trans J Robot Autom 5(3):269–279

Gabriele W, Renate S (2009) Work loss following stroke. J Disabil Rehabil 31(18):1487–1493

Han J, Qiu D, Song S (2012) Electronic nose to detect flavor substances fermented using plant lactobacillus in grass carp. J Food Sci 33(10):208–211 (in Chinese)
Liang Wei, Zhang L, Wang H et al (2013) Wine classification detection method based on the technology of electronic nose. J Sci Technol Eng 13(4):930–934 (in Chinese)
Lyle RC et al (1981) A performance test for assessment of upper limb function in physical rehabilitation treatment and research. J Int J Rehabil Res 4(4):483–492
Li N et al. (2011) Study on the forecast and prevention of waterqnrush from the lower-group coal floor in Zhaoguan coal mine. Shandong University of Science and Technology, Qingdao (in Chinese)
Jakel R, Schmidt-Rohr SR, Losch M, Dillmann R (2010) Representation and constrained planning of manipulation strategies in the context of programming by demonstration. In: Proceedings of the IEEE international conference robotics and automation (ICRA), pp 162–169
Jakel R, Schmidt-Rohr SR, Xue Z, Losch M, Dillmann R (2010) Learning of probabilistic grasping strategies using programming by demonstration. In: Proceedings of the IEEE international conference on robotics and automation, ICRA
Jäkel R, Schmidt-Rohr SR, Rühl SW, Kasper A, Xue Z, Dillmann R (2012) Learning of planning models for dexterous manipulation based on human demonstrations. Int J Soc Robot 4:437–448
Meng H et al (2010) Handle pressure distribution test system based on LabVIEW. Zhejiang University of Technology, Hangzhou (in Chinese)
Meng D, Xu G et al (2013) The research progress of upper limb function assessment tools in patients with hemiplegia. J Chin J Rehabil Theor Pract 38(7):1032–1035 (in Chinese)
Nathan DE, Johnson MJ, McGuire JR (2009) Design and validation of low-cost assistive glove for hand assessment and therapy during activity of daily living-focused robotic stroke therapy. J Rehabil Res Dev 46(5):587–602
Palm R, Iliev B (2014) Programming by demonstration and adaptation of robot skills by Fuzzy time modeling. J Appl Mech Mater:648–656
Palm R, Iliev B, Kadmiry B (2010) Grasp recognition by Fuzzy modeling and hidden Markov models. In: Programming-by-demonstration of robot motions
Skoglund A, Iliev B, Palm B (2010) Programming by demonstration of reaching motions a next state planner approach. J Robot Auton Syst 58(5):607–621
Song C et al (2013) Study on motion control and stably grab of for arm-hand system. Hunan University, Changsha (in Chinese)
Weng C, Wang J, Wang G et al (2007) Reliability of the action research arm test in stroke patients. J China Rehabil Theor Pract 13(9):868–869 (in Chinese)
Yozbatiran N, Der-Yeghiaian L, Cramer SC (2008) A standardized approach to performing the action research arm test. J Neurorehabil Neural Repair 22(1):78–90
Zampieri C, Salarian A, Carlson-Kuhta P et al (2011) Assessing mobility at home in people with early Parkinson's disease using an instrumented timed Up and Go test. J Parkinsonism Relat Disord 17(4):277–280

An Emotion Recognition System Based on Physiological Signals Obtained by Wearable Sensors

Cheng He, Yun-jin Yao and Xue-song Ye

Abstract Automatic emotion recognition is a major topic in the area of human–robot interaction. This paper presents an emotion recognition system based on physiological signals. Emotion induction experiments which induced joy, sadness, anger, and pleasure were conducted on 11 subjects. The subjects' electrocardiogram (ECG) and respiration (RSP) signals were recorded simultaneously by a physiological monitoring device based on wearable sensors. Compared to the non-wearable physiological monitoring devices often used in other emotion recognition systems, the wearable physiological monitoring device does not restrict the subjects' movement. From the acquired physiological signals, one hundred and forty-five signal features were extracted. A feature selection method based on genetic algorithm was developed to minimize errors resulting from useless signal features as well as reduce computation complexity. To recognize emotions from the selected physiological signal features, a support vector machine (SVM) method was applied, which achieved a recognition accuracy of 81.82, 63.64, 54.55, and 30.00 % for joy, sadness, anger, and pleasure, respectively. The results showed that it is feasible to recognize emotions from physiological signals.

Keywords Emotion recognition · Physiological signals · Wearable sensors · Genetic algorithm · Support vector machine

1 Introduction

Automatic emotion recognition is a major topic in the area of human–robot interaction. People express emotions through facial expressions, tone of voice, body postures, and gestures which are accompanied with physiological changes. Facial expressions, tone of voice, body postures, and gestures are controlled by the

C. He · Y. Yao · X. Ye (✉)
Department of Biomedical Engineering and Instrument Science,
Zhejiang University, 310027 Hangzhou, China
e-mail: yexuesong@zju.edu.cn

© Zhejiang University Press and Springer Science+Business Media Singapore 2017

C. Yang et al. (eds.), *Wearable Sensors and Robots*, Lecture Notes in Electrical Engineering 399, DOI 10.1007/978-981-10-2404-7_2

somatic nervous system while physiological signals, such as electroencephalogram (EEG), heart rate (HR), electrocardiogram (ECG), respiration (RSP), blood pressure (BP), electromyogram (EMG), skin conductance (SC), blood volume pulse (BVP), and skin temperature (ST) are mainly controlled by the autonomous nervous system. That means facial expressions, tone of voice, body postures, and gestures can be suppressed or masked intentionally while physiological signals can hardly be masked. Using physiological signals to recognize emotions is also helpful to those people who suffer from physical or mental illness thus exhibit problems with facial expressions, tone of voice, body postures or gestures.

Researches have shown a strong correlation between emotions and physiological signals. However, whether it is reliable to recognize emotions from physiological signals is still problematic. Numerous researches were investigating the problem (Picard et al. 2001; Lisetti and Nasoz 2004; Kim and André 2008; Rattanyu et al. 2010; Verma and Tiwary 2014).

This paper presents an emotion recognition system based on physiological signals obtained by wearable sensors. Some common emotion models and emotion induction methods are described briefly. The data collection procedure during which a physiological monitoring device based on wearable sensors was used is introduced. The strategy for feature extraction from the acquired physiological signals and the feature selection method based on genetic algorithm are illustrated. The support vector machine (SVM) method which was used to classify the physiological features into four kinds of emotions is demonstrated. The experiment implementation procedure is presented as well. Finally, the results of the experiments are discussed, which contribute to a conclusion.

2 Method

2.1 Emotion

In discrete emotion theory, all humans are thought to have an innate set of basic emotions that are cross-culturally recognizable (Ekman and Friesen 1971). In dimensional emotion theory, however, emotions are defined according to multiple dimensions (Schlosberg 1954). Although it is problematic which emotions are basic in discrete emotion theory (Gendron and Barrett 2009) and in which dimensions emotions should be defined in dimensional theory (Rubin and Talarico 2009), it's no doubt that joy, sadness, anger, and pleasure are four different common emotions in humans. Those four emotions were chosen as the classification categories in our study.

To obtain the physiological signals associated with the specific emotions, an effective emotion induction procedure is of significance. Numerous emotion or mood induction procedures (MIPs) have been reported including presenting subjects with emotional stimuli (pictures, film clips, etc.), and letting subjects play

games (van't Wout et al. 2010) or interact with human confederate (Kučera and Haviger 2012). Several picture, audio, or video databases for emotion induction have also been created (Biehl et al. 1997; Bai et al. 2005; Bradley and Lang 2008).

In our study, we did not use the emotion induction materials from those databases above because those materials did not induce the expected emotions effectively in our experiments. Instead, we selected several contagious video clips which performed better in our emotion induction experiments.

2.2 *Physiological Signals Processing*

2.2.1 Data Collection

Several kinds of physiological signals including ECG and RSP signals have been revealed to be correlated with emotions. To collect ECG and RSP signals, a physiological monitoring device based on wearable sensors which monitors multiple physiological signals simultaneously in real time (Zhou et al. 2015) was used. The ECG signals were sampled at 250 Hz and the RSP signals were sampled at 10 Hz. The schematic representation of a normal ECG waveform is shown in Fig. 1 and the ECG and RSP waveforms obtained by the physiological monitoring device are shown in Figs. 2 and 3, respectively.

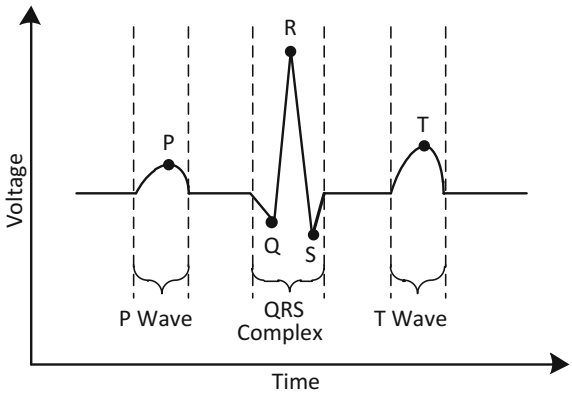

Fig. 1 Schematic representation of a normal electrocardiogram (ECG) waveform. An ECG waveform consists of a P wave, a QRS complex and a T wave. The QRS complex usually has much larger amplitude than the P wave and the T wave. P is the peak of a P wave. Q is the start of a QRS complex. R is the peak of a QRS complex. S is the end of a QRS complex. T is the peak of a T wave

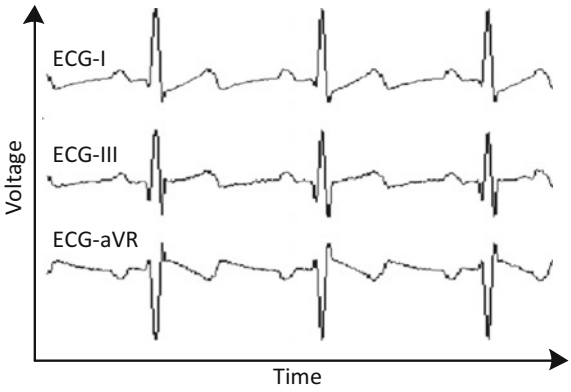

Fig. 2 Electrocardiogram (ECG) signals obtained by the physiological monitoring device. ECG-I is the voltage between the left arm electrode and right arm electrode. ECG-III is the voltage between the left leg electrode and the right leg electrode. ECG-aVR is the voltage between the right arm electrode and the combination of the left arm electrode and the left leg electrode

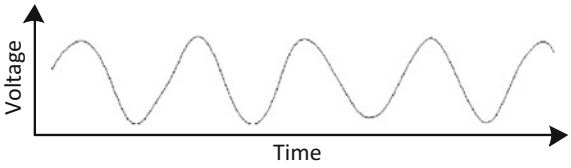

Fig. 3 Respiration (RSP) signals obtained by the physiological monitoring device

2.2.2 Feature Extraction

After the P-waves, the QRS complexes, and the T waves of the ECG signals were determined, a total of 78 ECG signal features were extracted as follows:

1. The mean value, median value, standard variance, minimum value, maximum value, and value range of R–R, P–P, Q–Q, S–S, T–T, P–Q, Q–S, and S–T time intervals;
2. The mean value, median value, standard variance, minimum value, maximum value, and value range of the amplitudes of P waves, QRS complexes, and T waves divided by the mean value of the corresponding ECG waveforms;
3. The mean value, median value, standard variance, minimum value, maximum value, and value range of HRD (the histogram distribution of R-R time intervals);
4. HR50 (the number of pairs of adjacent R-R time intervals differing by more than 50 ms divided by the total number of R-R time intervals);
5. HRDV (sum of HRD divided by the maximum value of HRD)
6. Each spectrum power of ECG signals in four frequency band (0–0.2 Hz, 0.2–0.4 Hz, 0.4–0.6 Hz, and 0.6–0.8 Hz).

Before RSP features were extracted, a low-pass filter was applied to the raw RSP signals. After that, a total of 67 RSP signal features were extracted as follows:

1. The mean value, median value, standard variance, minimum value, maximum value, value range, and peak ratio (the number of peaks divided by the length of data) of the following signals:
   (a) RSP waves, RSP peak–peak intervals, and RSP peak amplitudes;
   (b) The first difference of RSP waves, RSP peak-peak intervals, and RSP peak amplitudes
   (c) The second difference of RSP waves, RSP peak-peak intervals, and RSP peak amplitudes
2. Each spectrum power of RSP signals in four frequency band (0–0.1 Hz, 0.1–0.2 Hz, 0.3–0.3 Hz, and 0.3–0.4 Hz).

Considering the seventy-eight ECG signal features and the sixty-seven RSP signal features, a total of one hundred and forty-five features were extracted.

2.2.3 Feature Selection

More features usually provide more information about the original signals, but also lead to an increase in computational complexity. Besides, the random noise in those signal features which make little contribution to identify different emotions might leads to overfitting in supervised machine learning such as SVM. Therefore, an effective feature selection method to select only a key subset of measured features to create a classification model is needed. Emotion recognition can be looked as a pattern recognition issue. For a pattern recognition issue, the selection criterion usually involves the minimization of a specific measure of predictive error for models which fit to different subsets. A common method is sequential feature selection (SFS) (Cover and Van Campenhout 1977), which adds features from a candidate subset while evaluating the criterion. Another novel method is using genetic algorithm (Deb et al. 2002) to select features, which will be described here.

The genetic algorithm (GA) is a method based on natural selection which drives biological evolution. The GA repeatedly modifies a population of individual solutions. At each step, the GA selects individuals at random from the current population to be parents and uses them to produce the children for the next generation. There are some rules like crossover at each step to create the next generation from the current population. At each step, the individual selection is random, but the survival opportunity of each individual is not equal. The individuals who have higher survival opportunity are more likely to be selected and keep evolving till the optimization goal is reached. In our study, the survival opportunity was evaluated by the emotion recognition error.

Through the GA algorithm described above, fourteen features were selected from the original one hundred and forty-five features.

2.3 Emotion Recognition

To recognize emotions from the key features selected by GA, a modified support vector machine (SVM) method was used. An SVM classifies data by finding the optimal hyperplane that separates all data points of one class from those of another class (Cortes and Vapnik 1995). The optimal hyperplane for an SVM means the one with the maximum margin between the two classes. A margin is the maximal width of two slabs parallel to the hyperplane that have no interior data points. A larger margin assures the hyperplane is more likely to classify new data correctly. The data points that are on the boundary of the slab are called support vectors. The complexity of the classifier is characterized by the number of support vectors rather than the dimensionality of the transformed hyperspace. An example of SVM is shown in Fig. 4.

Sometimes the data might not allow for a separating hyperplane. As shown in Fig. 5, the outliers caused by error such as artifact during data collection make it difficult to find a proper separating hyperplane. Even if a separating hyperplane is found, the margin is small. In that case, a soft margin method is proposed which chooses a hyperplane that splits the examples as cleanly as possible while still maximizing the distance to the nearest cleanly split (Cortes and Vapnik 1995).

Some binary classification problems do not have an effective linear separating hyperplane, so-called nonlinear classification, as shown in Fig. 6a. In this case, the initial hyperspace S is transformed to a higher dimensional hyperspace S', as shown in Fig. 6b. In the higher dimensional hyperspace S', there is a linear hyperplane to successfully separate the two classes. Usually, the analysis formula of the

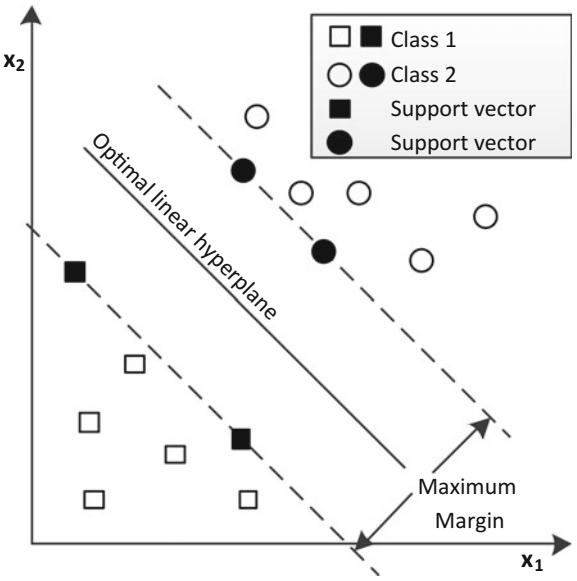

Fig. 4 Linear Support vector machine. The optimal linear hyperplane separates all samples into two classes with a maximum margin